Biophysical Chemistry, 47 (1993) 225–232
Elsevier Science Publishers B.V., Amsterdam

BIOCHE 01769

Thermodynamic parameters of cooperative helix-to-coil transitions from synthetic A–U-rich oligoribonucleotides up to fourteen basepairs

N. Windhab *, J. Ohms and Th. Ackermann

Institut für Physikalische Chemie, Universität Freiburg, Albertstr. 23a, D-7800 Freiburg (FRG)

(Received 26 October 1992; accepted in revised form 11 March 1993)

Abstract

Heat induced helix-to-coil transitions are studied in the form of ultraviolet-hypochromicity profiles by absorbance spectroscopy, and ΔC_p-curves by differential scanning calorimetry of self-complementary ribonucleotides. The results are analyzed and compared. Van 't Hoff transition enthalpies derived by UV-experiments incorporating concentration variations are found to differ from six-parameter and two-parameter Marquardt-fits on the melting profiles. A measure for the maximum number of nucleotides in intermediate states is obtained from a statistical deconvolution. It yields a range from 12.5% for the shortest nucleotide up to 31.5% for $r(UA)_7$. Model independent calorimetric data are reported. A limit for intra-molecular loop-formation preference is reached by $rG(UA)_6C$ within this sequence.

Keywords: A–U-rich oligoribonucleotides; Ultraviolet absorption spectroscopy; Marquardt-fit; Differential scanning calorimetry; DSC-deconvolution; Loop-formation

1. Introduction

Fast and sophisticated algorithms to calculate oligo- and polynucleotide secondary structure derive with some success a theoretical minimization of energy by effective selection of basepairing [1–3]. This estimation of complex properties depends on the quality of its set of nearest-neighbour parameters. Some sets of parameters are commonly applied and they are constantly improved [4–6]. Still further measurements are in request. New studies show that different sequence dependent elements of secondary structure occur in addition to classical basepairing as for example hydrogen bonds with the backbone in hairpin loops or unusual basepairing [7,8,20].

In order to refine thermodynamic parameters and to exclude unclassical behaviour this study compares further self-complementary ribonucleotides. In addition to the most common evaluation of transition parameters by ultraviolet melting-profiles we measured excess-enthalpies by model-independent calorimetric experiments (DSC), evaluated the size of the cooperative unit and deconvoluted the shape of the ΔC_p-curve [12]. This leads to a specific interpretation of the UV-experiment. The comparison of alternating

* To whom correspondence should be addressed.

and non-alternating A–U-systems gives a favorable statement for the nearest-neighbour approximation for these systems up to terminal G–C-basepairs and loop formation.

2. Materials and methods

2.1 Preparation of rA_6U_6; $r(UA)_n$, $n = 5–7$; $rG(UA)_iC$, $i = 4–6$ and $rG(AU)_5C$

An enzymatic synthesis by rA_6 and UDP as described by Breslauer et al. led to rA_6U_6 [9]; the alternating oligomers were obtained from the synthesizer by the method of Usman et al. [10]. All chemicals for the enzymatic synthesis were purchased from Boehringer (Mannheim), the monomers for alternating synthesis were purchased from Milligen (Eschborn). An Applied Biosystems 380 A-system was used for synthesis. The products were characterized by polyacrylamide gel-electrophoresis and quantitative FT-IR spectroscopy in the 1750–1550 cm^{-1}-region (D_2O) (Bruker IFS 113v-spectrometer).

The preparative isolation was carried out on a Fractogel TSK DEAE-650(S) (Merck) MPLC-column as described by Rockstroh and Wangler [11]. The separation from the reaction-compounds was achieved by a linear concentration gradient at pH 10.4 in 10 m*M* Tris from 0.1–0.6 *M* KCl (2 × 1000 ml). Figure 1 shows the profile of elution of fully deprotected $r(UA)_6$. The fraction was desalted by a TEAB-batch procedure on Fractogel. TEAB was eliminated by three-time rotary evaporation and resolution. Traces of salt and TEAB were eliminated by gel-filtration through a Sephadex G-10 column (Pharmacia) [12].

2.2 Sample preparation

All measurements reported were performed in buffer solutions containing 1 *M* NaCl, 0.01 *M* sodium phosphate and 10^{-4} *M* EDTA at pH 7. Defrosted or resolved probes containing G–C-sequences exhibited reversibility after being heated one time up to 95°C. All concentrations were determined spectroscopically. A semi-empirical method used nucleotide increments compiled by Borer et al. to calculate extinction coefficients at 25°C as shown in Table 1 [13].

2.3 UV-experiments

Nucleotide concentrations and ultraviolet melting profiles were recorded with a Perkin-Elmer Lambda 7 UV/VIS spectrometer at the absorption maximum near 260 nm. The melting profile was recorded on an analog *x–y* plotter and digitalized, the temperature was measured in the reference-cell. The heating rate was 1°C/min

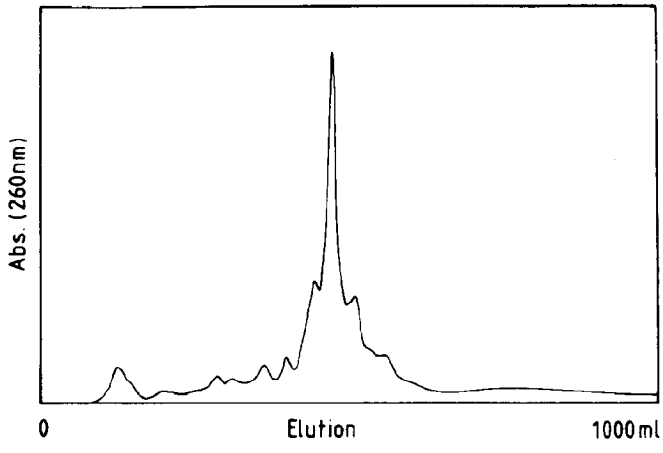

Fig. 1. Elution profile of reaction-compounds for 1 μmol $r(UA)_6$ which was isolated on a Fractogel TSK DEAE-650(S) MPLC-column by a linear KCl-gradient 0.1–0.6 *M* (2 × 1000 ml) at pH 10.4 to avoid secondary structure effects.

Table 1

Extinction coefficients ε of the oligomers at 260 nm and 25°C

Nucleotide	ε (M^{-1} cm^{-1})
rA_6U_6	11040
$r(UA)_5$	11780
$r(UA)_6$	11760
$r(UA)_7$	11740
$rG(UA)_4C$	11140
$rG(UA)_5C$	11230
$rG(AU)_5C$	11190
$r(UA)_3GC(UA)_3$	11210
$rG(UA)_6C$	11290

in a range of 5 to 75°C. Each sample exhibited high reversibility, samples which did not regain their 25°C-absorption after the melting experiment were not used.

2.4 Differential scanning calorimetry

DSC experiments were carried out with the DASM-4 calorimeter (V/O Mashbriborintorg USSR) (for a review see [14]). The active size of the cell is 0.47 ml; the required sample size is 0.9 ml. The absolute enthalpic effects which could be evaluated by these transitions were in the mJoule region, thus the nucleotide fraction contained more than 15 OD. Heating rate was 1°C/min and the 25°C-absorption was checked after melting experiments. All experiments were carried out three times and the results averaged.

3. Results

3.1 Optically derived thermodynamic parameters

Homologous selfcomplementary A–U-oligonucleotides with a chain length shorter than 20 bp form double helical structures [15]. The bimolecular formation is concentration-dependent. If an "all-or-none" process with a degree of transition α is presumed the sigmoidial transition profile of the hypsochromic effect depends on the van 't Hoff enthalpy $\Delta H^{uv}_{v.H.}$ and the total strand concentration C_t according to the equations [16]

$$\Delta H^{uv}_{v.H.} = 6RT^2 \left(\frac{\partial \alpha}{\partial T} \right)_{T_m} \quad (1)$$

$$\frac{1}{T_m} = \frac{R}{\Delta^{uv}_{v.H.}} \ln C_t + \frac{\Delta S}{\Delta H^{uv}_{v.H.}} \quad (2)$$

with T_m at $\alpha = 0.5$.

T_m was evaluated by a normalisation of the UV-melting profile. A simple linear regression using a few pairs of data lying outside of the transition area was applied to find the asymptotes. Figure 2 shows the measured concentration dependence of $1/T_m$ for $r(UA)_6$ in the upper line.

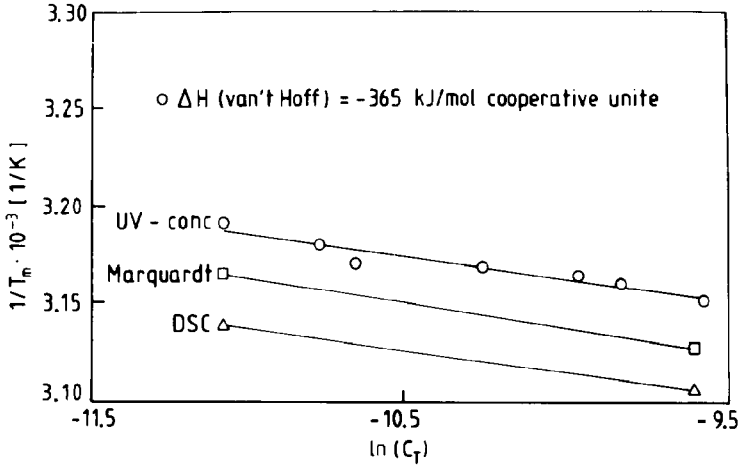

Fig. 2. $1/T_m$ vs. ln C_t of $r(UA)_6$ by several methods.

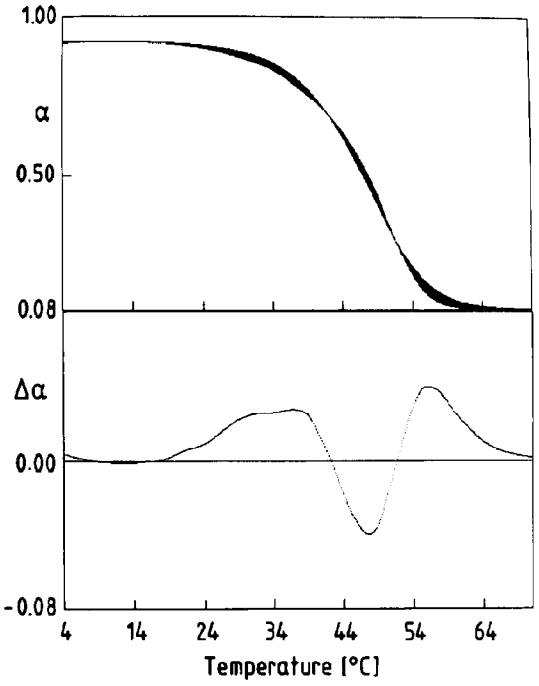

Fig. 3. Least-squares fit of the UV-melting-profile of $rG(AU)_5C$ in 1 *M* NaCl at pH 7 as a normalized α(T)-curve and an "all-or-none" transition. The lower part shows the typical shape of the minimized difference between the experimental and simulated degree of transition $\Delta\alpha(T)$. Pure UA-sequences showed a 50% lower amplitude.

Since the results for T_m and thus $\Delta H_{v.H.}$ being sensitive to the choice of the basepoints for the regression, a χ^2-minimization routine according to Levenberg and Marquardt was programmed [18]. In order to express the sigmoidal transition as well as the asymptotic nature of the temperature dependence and of the single-(ss) and double-strand (ds) extinction, a six-parameter model was used:

$$E = \alpha(m_{ds}T + b_{ds}) + (1-\alpha)(m_{ss}T + b_{ss}), \quad (3)$$

$$K = \frac{\alpha}{2C_t(1-\alpha)^2}. \quad (4)$$

The normalized $\alpha(T)$-plots were aligned by a similar two-parameter routine. The results of both procedures converge towards simulated curves.

These procedure yield significantly different values in comparison with the common indirect methods according to eq. (1) and (2). Figure 3 shows a typical result of a two-parameter fit. The area between the theoretical curve and the experimental curve is shaded. Similar differences have been reported by Longfellow et al. [17], where previously good agreement had been assumed. The lower part of Fig. 3 represents the difference between the curves $\Delta\alpha(T)$.

The different results are indicated by small but crucial differences of the curves. Although all goodness-of-fit *R*-factors seemed to be quite small T_m and $\Delta H_{v.H.}$ and the transition entropy ΔS depend on the accuracy of the asymptotes. The transition curve is asymmetric which causes a further uncertainty in their position. The effect of

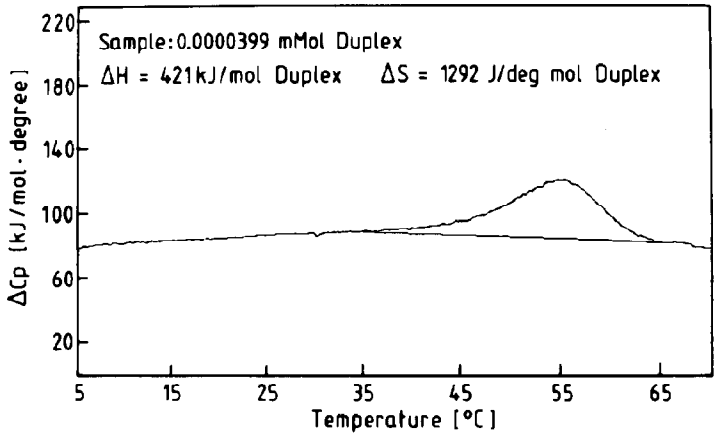

Fig. 4. DSC transition curve of the nucleotide $rG(UA)_5C$ in 1 *M* NaCl, pH 7. The transition enthalpy is registered differentially as $\Delta C_p(T)$. The chosen integration boarder is indicated.

Table 2

A comparison of the van 't Hoff enthalpies $\Delta H_{v.H.}$ (kJ/cooperative unit) derived by several methods. UV-experiments: concentration-dependent T_m-estimation, Marquardt-fit and calorimetry (DSC)

Nucleotide	$-\Delta H_{v.H.}$ (kJ/mol cooperative unit)		
	UV	UV-Marquardt	DSC
rA_6U_6	384	298	375
$r(UA)_5$	280	261	309
$r(UA)_6$	365	277	349
$r(UA)_7$	394	312	418
$rG(UA)_4C$	371	302	351
$rG(UA)_5C$	398	310	425
$rG(AU)_5C$	412	321	433
$r(UA)_3GC(UA)_3$	533	341 (566)	483
$rG(UA)_6C$	no concentration dependence of T_m		

the concentration on T_m as calculated by the algorithm is shown in Fig. 2 as the middle plot for $(UA)_6$ as one of our best fits.

3.2 Model-independent parameters

Figure 4 is the typical differential $\Delta C_p(T)$-plot of a helix-to-coil transition of $rG(UA)_5C$, also showing the asymmetrical transition. By integrating the curve a real heat of transition ΔH^{cal} per sample size was obtained. The same integration leads to the $\Delta\alpha(T)$-curve which can be interpreted by eq. (1) yielding a $\Delta H^{cal}_{v.H.}$ derived from calorimetric data.

The plot of eq. (2) using the calorimetric data is compared with the optical results in Fig. 2. Table 2 compares the different values of $\Delta H_{v.H.}$. While the Marquardt-routine appears to produce an average linear relation the normalisation by regression of asymptotes shows the correct $\Delta H_{v.H.}$. Thus a straightforward regression neglecting the assumption of the six-parameter model gives a consistent shift of T_m. This is why our fitted parameters can be improved by cutting the asymptotic parts by neglegting the basic model. This procedure was adopted for the nucleotide with highest cooperative "melting" of $(UA)_3GC(UA)_3$. The value is mentioned in Table 2 in brackets. The constant $\Delta S/\Delta H_{v.H.}$ in eq. (1) is a function of two observables. This causes the divergence in Fig. 2.

A model-independent transition entropy ΔS can be calculated by the integral

$$\Delta S^{cal} = \int_{T_0}^{T_n} \frac{C_p}{T} dT. \qquad (5)$$

Thus, the complete set of transition parameters listed in Table 3 is obtained. The length of the cooperative unit $\lambda = \Delta H_{v.H.}/\Delta H^{cal}$ as a measure of cooperativity in large aggregates is a function of intermediates, higher aggregates and the length

Table 3

Calorimetric and model-independent thermodynamic parameters of thermally induced reversible denaturation of self-complementary nucleotides. In contrast to shorter nucleotides all values of $rG(UA)_6C$ belong to a hairpin-loop denaturation

Nucleotide	$-\Delta H_{v.H.}$ (kJ/mol [a])	$-\Delta H$ (kJ/mol [b])	$-\Delta S$ (kJ/mol [b]·K)	$-\Delta G$ (37°C) (kJ/mol [b])	λ ($\Delta H_{v.H.}/\Delta H$)
rA_6U_6	375	348	1.09	10	1.08
$r(UA)_5$	309	281	0.88	8	1.1
$r(UA)_6$	349	338	1.06	9	1.03
$r(UA)_7$	418	415	1.28	18	1.01
$rG(UA)_4C$	351	350	1.09	12	1.01
$rG(UA)_5C$	425	418	1.28	21	1.02
$rG(AU)_5C$	433	414	1.27	20	1.05
$r(UA)_3GC(UA)_3$	483	449	1.34	33	1.08
$rG(UA)_6C$	169 [c]	171	0.52	10	0.98

[a] Mol cooperative unit.
[b] Mol duplex.
[c] This value is exclusively derived from the slope according to eq. (6).

Fig. 5. Secondary structure of rG(UA)$_6$C. The loop-region exerts no influence on the double-helical part which causes the total enthalpic stability.

of the nucleotide [12]. A value near unity does not indicate an "all-or-none" transition.

With rG(UA)$_6$C the behaviour changes. The data exhibits high thermodynamic stability with a T_m of 48.7°C, no concentration dependence and low enthalpic contribution. ΔH^{cal} reaches only 171 kJ and $\Delta H_{v.H.}$ is 169 kJ/mol which can be derived by

$$\Delta H^{uv}_{v.H.} = 4RT^2\left(\frac{\partial\alpha}{\partial T}\right)_{T_m} \tag{6}$$

assuming an intramolecular, unimolecular transition. Thus this oligoribonucleotide finds a favourable initial step to form a hairpin-loop. This domain cannot be formed with any shorter homologue or by the 14-mer without G–C-basepairs under these conditions. Figure 5 shows the most probable secondary structure, a simple addition of the stem increments gives excellent agreement assuming no enthalpic effect of the alternating pyrimidine–purine loop. A further IR-experiment indicated unstacked adenine residues even at low temperature. In natural RNA loops of this size are the most common.

3.3 DSC-deconvolution

The comparison of UV-results in Fig. 3 indicates a deviation from the fitted model in the transition area. The $\Delta C_p(T)$-curve can be deconvoluted in order to estimate the fraction of intermediates according to Freire and Biltonen [19], [12].

The fraction of fully double-helical aggregates will be

$$F_0 = \exp\left(-\int_{T_0}^{T}\frac{\langle H\rangle}{RT^2}\mathrm{d}T\right), \tag{7}$$

where $\langle H\rangle$ is the calorimetric heat contributed to the transition enthalpy up to the temperature T per mole double strand, and T_0 is a value for the starting point of the transition indicated by $\Delta\alpha(T)$. The fraction of completely denaturated nucleotides is

$$F_n = \exp\left(-\int_{T}^{T_n}(\Delta H^{cal} - \langle H\rangle)\frac{1}{RT^2}\mathrm{d}T\right), \tag{8}$$

where T_n is the assumed endpoint of transition from $\Delta\alpha(T)$. The amount of aggregates which do not participate in these "all-or-none" fractions are calculated by the summation

$$F_i = 1 - (F_0 + F_n). \tag{9}$$

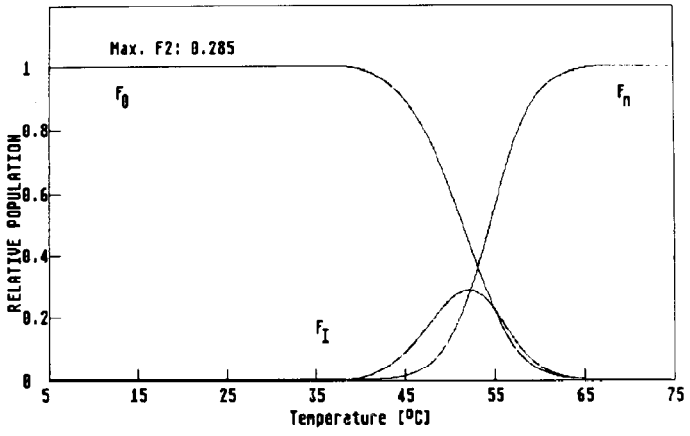

Fig. 6. DSC-deconvolution. Subtraction of the fraction calculated by an "all-or-none-transition" and the apparent enthalpic effect of rG(UA)$_5$C. In this case the maximum fraction exceeds 28%.

Table 4

Maximum fraction of intermediate by DSC-deconvolution. Note that a terminal G–C-basepair does not significantly suppress intermediates

Nucleotide	$F_{i,max}$ (%)
rA_6U_6	30
$r(UA)_5$	13
$r(UA)_6$	20
$r(UA)_7$	31
$rG(UA)_4C$	20
$rG(UA)_5C$	28.5
$rG(AU)_5C$	27
$r(UA)_3GC(UA)_3$	18
$rG(UA)_6C$	–

Figure 6 shows an example of this deconvolution. A initial approach will be to use the highest fraction of intermediates $F_{i,max}$ in Table 4 which is calculated from the condition of eq. (10).

$$\frac{\partial F_i(T)}{\partial T} = 0. \tag{10}$$

4. Discussion

The set of parameters offered in Table 3 gives a good agreement in the 5%-region of the rA_6U_6 melting behaviour and its alternating homologues which could not be expected. The same agreement is expressed by published parameters of shorter and longer non-alternating nucleotides in this series. With an enthalpic increment of about 29 kJ/mol, simple additive nearest-neighbour behaviour for an A–U-stem is probable. Since we find the same behaviour for $G(UA)_5C$ and $G(AU)_5C$, terminal G–C-basepairs appear to be simply added to the alternating A–U-nucleotides. Terminal G–C-basepairs increase thermal stability by an enthalpic effect of about 49 kJ/mol basepair. Even inner GC-basepairs show convincingly the same increment.

The interpretation of the UV melting-curves of the nucleotides is dependent on the chosen procedure. In this case goodness-of-fit pointers like R-factors are dependent on the temperature and transition interval, so they are relative values. The $\Delta\alpha(T)$-diagram, the lower part of Fig. 3 shows systematic divergence in the transition interval. The DSC-method registers a differential transition curve and enables a deconvolution. Even for the shortest nucleotides 12% of the intermediate states are populated during transition but no $\epsilon(T)$ for this fraction is available. A–U-rich nucleotides do not denature in an "all-or-none process". The strong GC-end does not affect this behaviour and "frays", causing its increased enthalpic effect. On the other hand, these basepairs join the cooperative melting-process of $(UA)_3GC(UA)_3$ and lower the percentage of intermediates. Pörschke et al. found an "all-or-none process" in their kinetic experiments on a shorter homologue with central GC bases [22].

For $G(UA)_6C$ the favourable entropy of an intramolecular folding exceeds the enormously unfavourable enthalpic lag of the intermolecular helix-formation at the same salt concentration. As no competitive transition can be detected by all the methods described, especially concentration independence of T_m a clear switch is achieved by exchanging the terminal A–U-pairs of $r(UA)_7$ for G–C. In addition longer A–U-nucleotides previously investigated do not form hairpin loops under these conditions [7,15].

A similar conclusion can be drawn with respect to the influence of enthalpic G–C-stabilization on intermediate populations. A good knowledge of synthetic stem-nucleotides leads to an understanding of the G–C-influence with respect to the enormous "intelligence" which natural DNA- and RNA-sequences do contain [8,20,21]. The small transition enthalpy of the $G(UA)_6C$ sample naturally lowers the calorimetric effect. This unfortunately caused too much uncertainty for any F_{max}-estimation. Further DSC and NMR experiments concerning transition intermediates and loop-formation will be reported.

Satisfactory yields and the purity of our products encourage works on oligoribonucleotides from the synthesizer using industrial monomeres with its obvious advantages for NMR-experiments or medical research.

Acknowledgements

We thank Dr. Gabor Igloi for the synthesis of the alternating sequences and all support by Mr. Willi Wangler. Discussion with Dr. Michael Grubert proved very useful. This work was supported by the Deutsche Forschungsgemeinschaft through SFB 60 (Teilprojekt H-1).

References

1 I. Tinoco, Jr., O.C. Ulhenbeck, and M.D. Levine, Nature 230 (1971) 362–336.
2 A. Wada, and A. Suyama, Prog. Biophys. Mol. Biol. 47 (1986) 113–157.
3 A. Malhotra, R.K.Z. Tan and S.C. Harvey, Proc. Natl. Acad. Sci. USA 87 (1990) 1950–954.
4 M. Zuker and P. Stiegler, Nucleic Acids Res. 9 (1981) 133–148.
5 Ch. Cheong, G. Varani and I. Tinoco, Jr., Nature 346 (1990) 680–682.
6 W. Salser, Harbor Symp. Quant. Biol. 62 (1977) 985–1002.
7 J. Ohms and Th. Ackermann, Biochemistry 29 (1990) 5237–5244.
8 S.M. Freier, R. Kierzek, J.A. Jaeger, N. Sugimoto, M.H. Caruthers, T. Neilson and D.H. Turner, Proc. Natl. Acad. Sci. USA 83 (1986) 9373–9377.
9 K.J. Breslauer, J.M. Sturtevant and J. Tinoco, J. Mol. Biol. 94 (1975) 549–556.
10 N. Usman, K.K. Oglivie, M.Y. Jiang and R.J. Cedergren, J. Am. Chem. Soc. 109 (1987) 7845–7854.
11 H. Rockstroh, W. Wangler and Th. Ackermann, J. Chromatogr. 442 (1988) 401–406.
12 J. Ohms and Th. Ackermann, Biophys. Chem., 34 (1989) 137–142.
13 P.N. Borer, in: Handbook of Biochemistry and Molecular Biology 3rd edn. vol. 1, Ed. G.D. Fasman (CRC Press, Cleveland, OH, 1975) p. 589.
14 Ackermann, Th., Angew. Chem., Int. Edn. 28 (1989) 981–991.
15 A.C. Dock-Bregeon, B. Chevrier, A. Podjarny, J. Johnson, J.S. de Bear, G.R. Gough, P.T. Gilham and D. Moras, J. Mol. Biol. 209 (1989) 459–474.
16 F.H. Martin, O.C. Uhlenbeck and P. Doty, J. Mol. Biol. 57 (1971) 201–215.
17 C.E. Longfellow, R. Kierzek and D.H. Turner, Biochemistry 29 (1990) 278–285.
18 W.H. Press, B.P. Flannery, S.A. Teukolsky and W.T. Veterling, Numerical recipes—The art of scientific computing (Cambridge University Press, 1981).
19 E. Freire and R.L. Biltonen, Biopolymers 17 (1978) 463–509.
20 G. Varani, Ch. Cheong, and I. Tinoco Jr, Biochemistry 30 (1991) 3280–3289.
21 P.H. van Knippenberg, J.M.A. van Kimmenade, and H.A. Heus, Nucleic Acids Res. 12 (1984) 2595–2604.
22 D. Pörschke, O.C. Uhlenbeck and F.H. Martin, Biopolymers 12 (1973) 1313–1335.